Direct chemoselective synthesis of glyconanoparticles from unprotected reducing glycans and glycopeptide aldehydes

Mikkel B. Thygesen, Kasper K. Sørensen, Emiliano Cló and Knud J. Jensen*

IGM -Bioorganic Chemistry, Centre for Carbohydrate Recognition and Signalling, Faculty of Life Sciences, University of Copenhagen, Thorvaldsensvej 40, DK-1871 Frederiksberg C, Denmark. Fax: +45 3533 2398; Tel: +45 3533 2430; E-mail: kjj@life.ku.dk

Supplementary Information

Table of contents:

I) Experimental Section

Materials and analysis. All chemicals and lectins were purchased from Sigma-Aldrich Denmark except for Fmoc-Ser(αGalNAc)-OH which was from Sussex Research, Canada. All chemicals were used as received without further purification. MilliQ water was used for aqueous preparations. All solvent ratios are v/v. ^{1}H, ^{13}C, APT, gHSQC, and H,H COSY NMR spectra were recorded on a Bruker Avance 300 spectrometer with a BBO probe. The chemical shifts are referenced to the residual solvent signal. Assignments were aided by H,H COSY, gHSQC, and APT experiments. Mass determinations (high resolution MS, HR-MS) were performed on a Micromass LCT instrument with an ESI probe. UV-Visible spectroscopy was recorded on a Jasco V-650 spectrophotometer. Analytical HPLC was performed on a Dionex Ultimate 3000 system with Chromeleon 6.80SP3 software; a linear gradient flow of MeCN-H_2O (0.1% formic acid) was used for separations on a C_4 (Jupiter, 5 μm, 300 Å, 150x4.6 mm) column from Phenomenex (Trim quantification). Transmission electron microscopy (TEM) was recorded on a Philips CM20 instrument at 200 keV. Dynamic light scattering measurements were performed on a BI-200SM instrument from Brookhaven Instruments Corporation. Microwave reactions were performed in a Biotage Initiator instrument. Transmission electron microscopy (TEM) measurements were recorded on a Philips CM20 instrument at 200 keV.

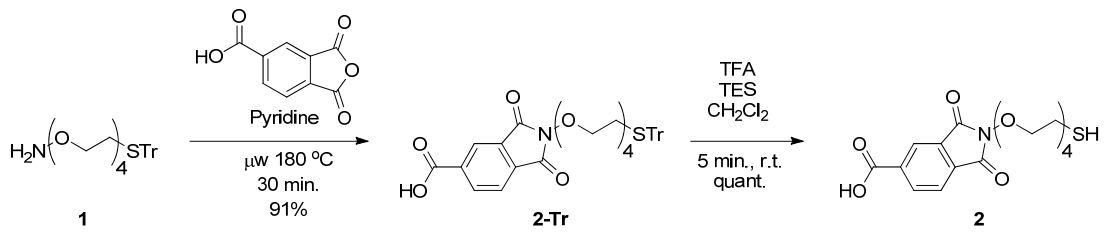

4-Carboxy-*N*-(2-{2-[2-(2-tritylsulfanylethoxy)ethoxy]ethoxy}ethoxy)phthalimide (**2-Tr**). *O*-(2-{2-[2-(2-Tritylsulfanylethoxy)ethoxy]ethoxy}ethyl)hydroxylamine **1** (47 mg, 0.1 mmol) was dissolved in dry pyridine (1 mL). Trimellitic anhydride (21 mg, 0.11 mmol) was added, and once dissolved, the reaction mixture was heated in a microwave reactor at 150 °C for 5 minutes, and then at 180 °C for 30 minutes. The reaction mixture was concentrated by rotary evaporation (oil pump) and co-evaporated twice with toluene. The residue was purified by vacuum liquid chromatography (VLC) (ethyl acetate-heptane 1:1→7:3 with 1% acetic acid) to provide 64 mg (91%) of the title compound as a thick, clear oil. ^{1}H NMR (300 MHz, $CDCl_3$): δ 8.49-8.47 (m, 1H; 3-*H* Trim), 8.45 (dd, *J*=7.7 and 1.4 Hz, 1H; 5-*H* Trim), 7.92 (dd, *J*=7.7 and 0.6 Hz, 1H; 6-*H* Trim), 7.43-7.36 (m, 6H; Tr meta), 7.30-7.15 (m, 9H; Tr ortho+para), 6.72 (br s, 1H; COO*H*), 4.41-4.35 (m, 2H;

C*H*$_2$ON), 3.89-3.84 (m, 2H; C*H*$_2$CH$_2$ON), 3.68-3.62 (m, 2H; C*H*$_2$OCH$_2$CH$_2$ON), 3.60-3.54 (m, 2H; C*H*$_2$CH$_2$OCH$_2$CH$_2$ON), 3.54-3.48 (m, 2H; C*H*$_2$CH$_2$OCH$_2$CH$_2$S), 3.45-3.39 (m, 2H; C*H*$_2$OCH$_2$CH$_2$S), 3.29 (t, *J*=6.9 Hz, 2H; C*H*$_2$CH$_2$S), 2.42 (t, *J*=6.9 Hz, 2H; C*H*$_2$S). ^{13}C NMR (75 MHz, $CDCl_3$): δ 168.2 (*C*OOH), 162.3 (*C*=O), 162.2 (*C*=O), 144.7 (Tr, ipso), 136.2 (Trim), 135.3 (Trim), 132.8 (Trim), 129.5 (Tr), 129.2 (Trim), 127.8 (Tr), 126.6 (Tr para), 124.9 (Trim), 123.6 (Trim), 77.3 (*C*H$_2$ON), 70.7, 70.4, 70.3, 70.0, 69.5, 69.3 (O*C*H$_2$CH$_2$STr), 66.5 (Tr quarternary), 31.5 (*C*H$_2$STr). HR-MS (ES): calcd for $C_{36}H_{35}NO_8S$ $[M+Na]^+$: 664.1981; found: 664.1975.

4-Carboxy-*N*-(2-{2-[2-(2-mercaptoethoxy)ethoxy]ethoxy}ethoxy)phthalimide (2). Compound **2-Tr** (39 mg, 0.06 mmol) was dissolved in dichloromethane (1 mL) under argon. Triethylsilane (0.25 mL) was added, followed by a dropwise addition of trifluoroacetic acid (0.5 mL) under stirring. A transient yellow color was observed during the addition, however, the reaction mixture was a clear solution after completion of the addition. The reaction mixture was stirred at room temperature for 5 minutes and then concentrated by rotary evaporation. The residue was purified by liquid-solid extraction with n-heptane (3x1 mL). Evaporation to dryness provided the desired thiol as a thick clear oil in quantitative yield. ^{1}H NMR (300 MHz, $CDCl_3$): δ 8.49-8.47 (m, 1H; 3-*H* Trim), 8.47-8.44 (m, 1H; 5-*H* Trim), 7.96-7.91 (m, 1H; 6-*H* Trim), 6.68 (br s, 1H; COO*H*), 4.43-4.37 (m, 2H; C*H*$_2$ON), 3.91-3.85 (m, 2H; C*H*$_2$CH$_2$ON), 3.71-3.65 (m, 2H), 3.65-3.55 (m, 8H), 2.72-2.63 (m, 2H; C*H*$_2$S), 1.57 (t, *J*=8.2 Hz, S*H*). ^{13}C NMR (75 MHz, $CDCl_3$): δ 168.1 (*C*OOH), 162.3 (*C*=O), 162.2 (*C*=O), 136.2 (Trim), 135.5 (Trim), 132.8 (Trim), 129.2 (Trim), 124.9 (Trim), 123.6 (Trim), 77.3 (*C*H$_2$ON), 72.8 (OC*H*$_2$CH$_2$SH), 70.7, 70.4, 70.4, 70.1, 69.3, 24.1 (C*H*$_2$SH). HR-MS (ES): calcd for $C_{17}H_{21}NO_8S$ $[M+Na]^+$: 422.0886; found: 422.0867.

Self-assembly of Trim-protected OEG linker 2 on gold nanoparticles (3). A solution of thiol **2** (24 mg, 0.06 mmol) in methanol (5 mL) was added to a 20 nM solution of ~12 nm citrate stabilized gold nanoparticles (60 mL, 1.2 nmol). A swift color change towards purple (red shift) was visible upon the addition. The mixture was stirred at room temperature for 16 hours. Subsequently, the assembled gold nanoparticles were purified in 10 mL batches by centrifugal filtration (Millipore Amicon Ultra, 50 kDa cutoff) with five consecutive filtration and dilution (5 mL of 10 mM phosphate buffer pH 7.0, 10 times dilution) steps. After the final filtration, the nanoparticles were diluted with 10 mM phosphate buffer pH 7.0 (total volume of 400 µL) to provide final nanoparticle concentrations of 0.50 µM of Trim-protected AuNPs **3** (2.4 mL in total).

Deprotection of aminooxy-terminated OEG linkers on gold nanoparticles. Generation of aminooxy-terminated core-shell OEG-AuNPs (4). A series of deprotection reactions of variable

duration were performed: To Trim-protected aminooxy AuNPs **3** (200 µL, 0.1 nmol) was added a 1 mM aqueous solution of hydrazine hydrate (1.00 mL). The completely transparent red solution was shaken at room temperature over a period of 24 hours. The deprotection reaction was arrested via removal of the nanoparticles by centrifugal filtration (Millipore Amicon Ultra, 50 kDa cutoff). The filtrate was used for quantification of the released 6-carboxy-2,3-dihydrophthalazine-1,4-dione (see below). Subsequently, the aminooxy-terminated AuNPs were purified by five consecutive filtration and dilution (5 mL of 10 mM phosphate buffer pH 7.0, 10 times dilution) steps. After the final filtration, the nanoparticles were diluted with 10 mM phosphate buffer pH 7.0 (total volume of 400 µL) to provide final nanoparticle concentrations of 0.50 µM of aminooxy-terminated AuNPs **4**.

6-Carboxy-2,3-dihydrophthalazine-1,4-dione (5). Trimellitic anhydride (961 mg, 5.0 mmol) was dissolved in absolute ethanol (20 mL). Hydrazine hydrate (243 µL, 5.0 mmol) was added, and the reaction mixture was heated to reflux for 24 hours. The resulting suspension was filtered and dried under high vacuum (oil pump) to provide 844 mg (82%) of the title compound as a white solid. ^{1}H NMR (300 MHz, DMSO-D_6): δ 12.36 (br s, 3H; O*H*+2xN*H*), 8.58 (d, *J*=1.7 Hz, 1H; *H*-5), 8.33 (dd, *J*=8.3 and 1.7 Hz, 1H; *H*-7), 8.14 (br d, *J*=8.3 Hz, 1H; *H*-8). ^{13}C NMR (75 MHz, DMSO-D_6): δ 166.2 (*C*OOH), 154.9 (br, *C*=O), 154.0 (br, *C*=O), 134.1 (*C*-6), 132.5 (*C*-8), 129.6 (br, *C* ipso), 127.4 (br, *C* ipso), 126.5 (*C*-5), 125.7 (*C*-7). HR-MS (ES): calcd for $C_9H_5N_2O_4$ $[M+H]^+$: 207.0406; found: 207.0423.

Quantification of aminooxy OEG linker density on AuNPs 4. HPLC standard curves of 6-carboxy-2,3-dihydrophthalazine-1,4-dione **5** at 254 and 300 nm were generated from samples made from two 100 ppm stock solutions (1.00 mL of a 10.0 mg/mL solution in DMSO diluted to 100 mL with water). The injection volume was 20 µL. Aliquots of the filtrates from deprotection of aminooxy-OEG-AuNPs (200 µL) were allowed to stand at room temperature for 48 hours in closed vials. Subsequently, the filtrate was acidified with acetic acid (10 µL), and then injected (100 µL) into the HPLC system. Thus, the overall dilution factor (DF) was 0.21 (i.e. (210 µL/200 µL)*(20 µL/100 µL)), and the quantification volume, V_{quant}, was 1.20 mL (i.e. 200 µL nanoparticle solution+1.00 mL hydrazine solution).

Peptide aldehyde solid-phase synthesis. Peptide aldehydes were synthesized using an *o*-PALdehyde strategy[S1] on a TentaGel S-NH_2 0.26 mmol/g resin. Following automated standard solid-phase synthesis with N^{α}-Fmoc protected amino acids the peptides were purified by preparative C_4 RP-HPLC.

Fmoc-Glu-Glu-Gly-Gly-H: HR-MS (ES): calcd for $C_{29}H_{32}N_4O_{10}$ $[M+H]^+$: 597.2197; found: 597.2202.

Ac-Tyr-Gly-Ser(αGalNAc)-Glu-Gly-Gly-H: MS (ES): calcd for $C_{33}H_{47}N_7O_{16}$ $[M+H]^+$: 798.3; found: 798.3; calcd for $[M+2H]^{2+}$: 399.7; found: 399.7; calcd for $[M+3H]^{3+}$: 266.8; found 266.7.

General procedure for oxime coupling with peptide aldehydes on aminooxy-terminated core-shell AuNPs (6 and 8). A 2.5 mM solution of the peptide aldehyde Fmoc-Glu-Glu-Gly-Gly-H or glycopeptide aldehyde Ac-Tyr-Gly-Ser(αGalNAc)-Glu-Gly-Gly-H (200 μL, 500 nmol) in 10 mM phosphate buffer pH 7.0 was added to a 0.5 μM solution of aminooxy-terminated AuNPs **4** (200 μL, 0.1 nmol) in 10 mM phosphate buffer pH 7.0. The transparent, dark red reaction mixture was shaken at 40 °C for 16 hours. Subsequently, the peptide capped gold nanoparticles were purified by centrifugal filtration (Millipore Amicon Ultra, 50 kDa cutoff) with five consecutive filtration and dilution (5 mL of 10 mM phosphate buffer pH 7.0, 10 times dilution) steps. After the final filtration, the nanoparticles were diluted with 10 mM phosphate buffer pH 7.0 (total volume of 400 μL) to provide final nanoparticle concentrations of 0.50 μM of peptide-conjugated AuNPs **6** and **8**.

Fmoc deprotection on peptide-capped core-shell AuNPs and quantification (7). To Fmoc-protected peptide-conjugated AuNPs **6** (200 μL, 500 nmol) in 10 mM phosphate buffer pH 7.0 was added a 50 % aqueous solution of piperidine (0.8 mL). The transparent red reaction mixture was shaken at room temperature for 30 minutes, whereafter the nanoparticles were removed by centrifugal filtration (Millipore Microcon-YM, 30 kDa cutoff). The filtrate was transferred to a quatz cuvette (Helma QS 250), and the absorbance at 300 nm was measured (relative to a similarly treated sample, lacking the nanoparticles). $\varepsilon_{300\ nm}$=7800 $M^{-1}cm^{-1}$.

General procedure for oxime coupling with excess glycans on aminooxy-terminated core-shell AuNPs (conditions I; 9(conditions I) and 10(conditions I)).

A 1 M solution of the glycan (50 μL, 50 μmol) in 10 mM acetate buffer pH 4.7 was added to a 0.5 μM solution of aminooxy-terminated AuNPs **4** (50 μL, 0.025 nmol) in 10 mM phosphate buffer pH 7.0. The transparent, dark red reaction mixture was shaken at 40 °C for 16 hours. Subsequently, the glycan capped gold nanoparticles were purified by centrifugal filtration (Millipore Amicon Ultra, 50 kDa cutoff) with ten consecutive filtration and dilution (5 mL of 10 mM phosphate buffer pH 7.0, 10 times dilution) steps. After the final filtration, the nanoparticles were diluted with 10 mM phosphate buffer pH 7.0 (total volume of 400 μL) to provide final nanoparticle concentrations of 0.125 μM of glyconanoparticles **9**(conditions I) and **10**(conditions I).

General procedure for oxime coupling with glycans under nucleophilic catalysis on aminooxy-terminated core-shell AuNPs (conditions II; 9(conditions II), 10(conditions II), and 11(conditions II)).

A 10 mM solution of the glycan (50 μL, 500 nmol) in 10 mM acetate buffer pH 4.7 containing 10 mM 4-anisidine was added to a 0.5 μM solution of aminooxy-terminated AuNPs **4** (50 μL, 0.025 nmol) in 10 mM phosphate buffer pH 7.0. The transparent, dark red reaction mixture was shaken at 40 °C for 16 hours. Subsequently, the glycan capped gold nanoparticles were purified by centrifugal filtration (Millipore Amicon Ultra, 50 kDa cutoff) with five consecutive filtration and dilution (5 mL of 10 mM phosphate buffer pH 7.0, 10 times dilution) steps. After the final filtration, the nanoparticles were diluted with 10 mM phosphate buffer pH 7.0 (total volume of 400 μL) to provide final nanoparticle concentrations of 0.125 μM of glyconanoparticles **9**(conditions II), **10**(conditions II), and **11**(conditions II).

Lectin assays with glycan-conjugated AuNPs.

5 nM solutions of glyconanoparticles **8**, **9**,[S2] **9**(conditions I), **9**(conditions II), **10**(conditions I), **10**(conditions II), or **11**(conditions II) in phosphate buffer pH 7.0 were treated with a final concentration of 5.0 μM of either of Con A from *Canavalia ensiformis*, ECA from *Erythrina cristagalli*, or HAA from *Helix aspersa* by addition of 50 μM solutions in water at 25 °C. Aggregation was monitored by UV-Vis spectroscopy by measurement of the shifts in surface plasmon peak maximum, λ_{SP}, over periods of 4-6 hours.

II) Self-assembly of Trim-protected OEG linker 2 onto gold nanoparticles.

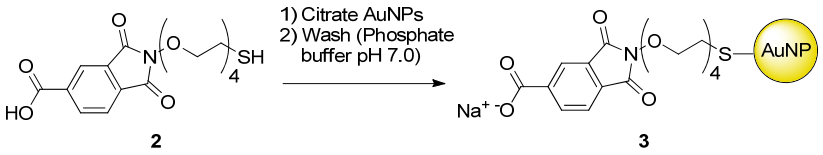

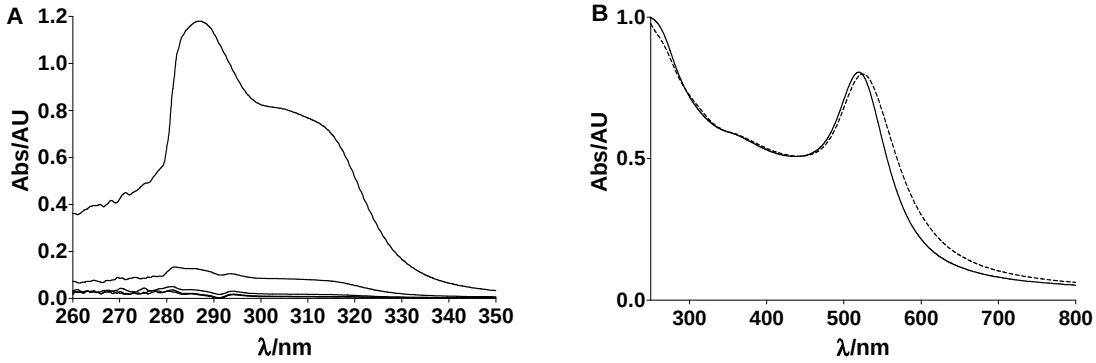

Self-assembly with Trim-protected OEG linker **2**. (A) UV-Vis spectra of five consecutive washing fractions from ligand exchange, (B) UV-Vis spectra of nanoparticles before (—) and after (**3**, ---) modification with Trim-protected OEG linker.

III) Calibration curve for 6-carboxy-2,3-dihydrophthalazine-1,4-dione (5).

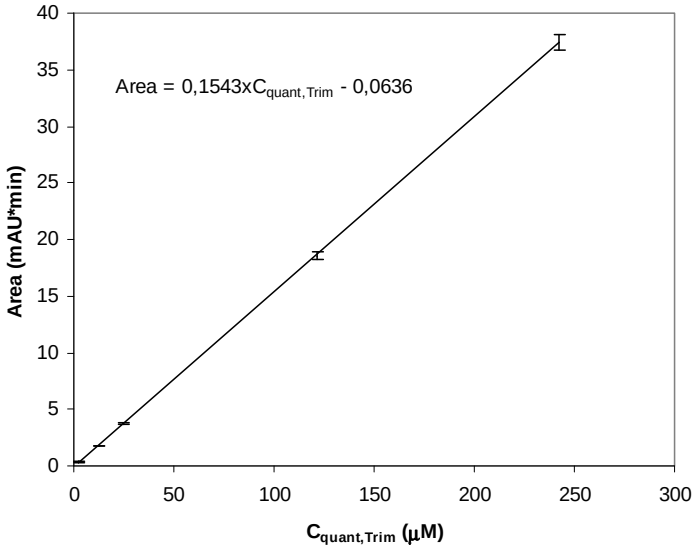

HPLC calibration curve for 6-carboxy-2,3-dihydrophthalazine-1,4-dione (**5**) at 254 nm. Samples were prepared and analyzed in duplicate.

IV) Quantification of Trim-cleavage from gold nanoparticles 3.

A series of cleavage experiments were performed by treatment of Trim-protected AuNPs **3** with 1 mM aqueous hydrazine. $C_{quant,Trim}$ values were determined from the HPLC areas of the released 6-carboxy-2,3-dihydrophthalazine-1,4-dione (**5**) via the calibration curve under III. The determined $C_{quant,Trim}$ values increased rapidly during the first couple of hours and leveled off at a value below 200 µM (approximately 40 ppm).

Quantification of linker density by measurement of released 6-carboxy-2,3-dihydrophthalazine-1,4-dione.[a]

Time (h)	Area (mAU*min)	$C_{quant,Trim}$ (µM)	*Linker density* (linkers/nanoparticle)	*Surface coverage* (linkers/nm^2)
0	0	0	0	0
1	10.8	70.3	177	0.36
2	15.3	99.7	251	0.50
16	25.0	163	410	0.82
17	25.8	168	422	0.85
24	26.6	173	437	0.88

[a] $C_{quant,Trim}$ values were found from the calibration curve of **5**.

From the quantified concentrations, $C_{quant,Trim}$, the linker density, i.e. the average number of linkers per nanoparticle, could be calculated based on the assumption that there were no changes in the size and/or concentration of the gold cores during the self-assembly and subsequent cleavage steps. This assumption was based on the very mild conditions of self-assembly and cleavage, and it was supported by the absence of a red-shift in the surface plasmon band after self-assembly and during cleavage. Furthermore, any aggregation or loss of material during workup would generally result in lowered *linker density* determinations. The *linker density* could be calculated as follows

$$Linker\ density = \frac{n_{quant,Trim}}{n_{citrate\ AuNPs}} = \frac{DF_{quant,Trim} \cdot C_{quant,Trim} \cdot V_{quant,Trim}}{n_{citrate\ AuNPs}}$$

where the dilution factor, $DF_{quant,Trim}$, was 0.21, the quantification volume, $V_{quant,Trim}$, was 1.2 mL, and the amount of gold nanoparticles, hence the amount of citrate stabilized gold nanoparticles, $n_{citrate\ AuNPs}$ was 0.1 nmol (see experimental section) in all entries of the table. The *linker density* approched 500 linkers/particle over the 24 hour period. The corresponding *surface coverage*, i.e. the

average geometrical area taken up by a single linker on the surface of an idealized spherical gold nanoparticle with a radius, $r_{particle}$, could be calculated as

$$Surface\ coverage = \frac{Linker\ Density}{4 \cdot \pi \cdot r_{particle}^2}$$

where $r_{particle}$ was 6.3 nm for the determinations in the table, as measured by transmission electron microscopy of the citrate stabilized gold nanoparticles.[S2]

V) UV-Vis spectra of Fmoc cleavage from AuNPs 6.

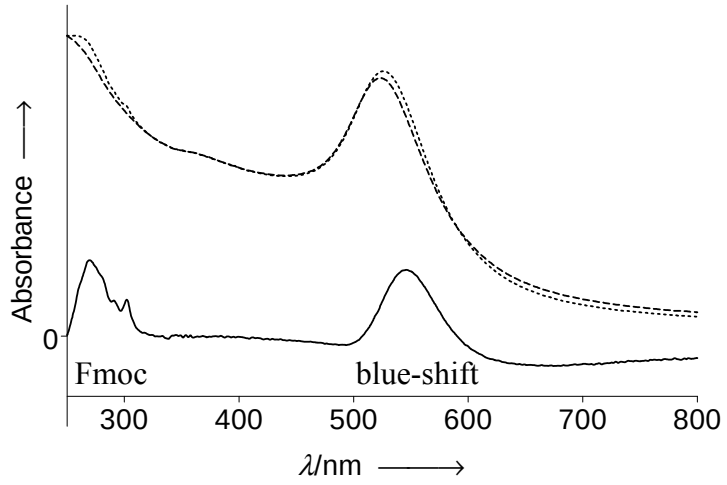

Normalized UV-Vis spectra of AuNPs before (**6**, ····) and after (**7**, ---) Fmoc deprotection. A subtraction (5x magnified) of the two spectra (—) clearly reveals a characteristic Fmoc signal as part of the spectrum of **6**. The Fmoc signal has characteristic maxima at 270, 291, and 300 nm. A slight blue-shift of ΔSP upon piperidine treatment (~3 nm) is manifested as a peak around 546 nm in the spectrum subtraction.

VI) Dynamic ligth scattering measurements on AuNPs 3, 4, and 6.

The hydrodynamic diameters, d(H), of the functionalized AuNPs were measured in order to corroborate the chemoselective coupling reaction.

AuNP preparation	Hydrodynamic diameter, d(H), (nm)	Polydispersity (%)
Citrate stabilized AuNPs	20.3	11
Trim-protected AuNPs (**3**)	26.7	14
Aminooxy-terminated AuNPs (**4**)	21.7	15
Fmoc-Glu-Glu-Gly-Gly-conjugated AuNPs (**6**)	29.9	21

VII) Comparison of UV-Vis spectra of citrate-AuNPs and AuNPs 3, 4, and 9(conditions I).

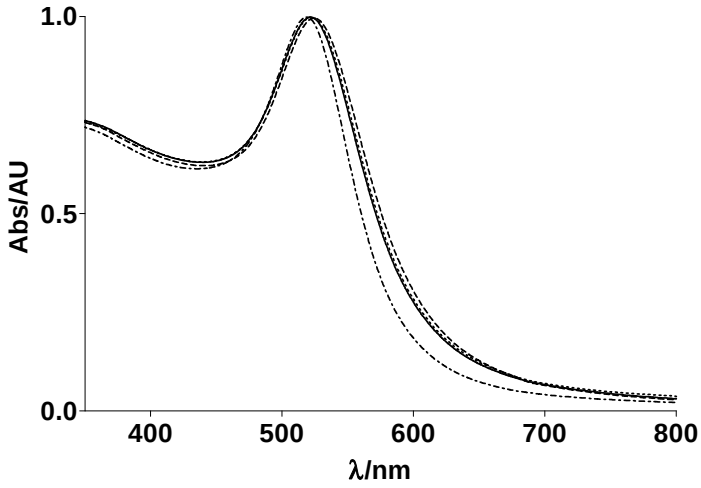

Overlay of normalized UV-Vis spectra of functionalization of core-shell AuNPs showing the minimal changes in SP band shape and maximum in going through the functionalization of citrate stabilized AuNPs (-···) with Trim-protected OEG linker (**3**, ---), and deprotection to aminooxy-terminated AuNPs (**4**, ····), and finally oxime coupling with maltose (**9**(conditions I), —).

VIII) Transmission electron microscopy analyses of citrate AuNps, and AuNPs 4 and 6.

Citrate AuNPs: AuNPs **4**: AuNPs **6**:

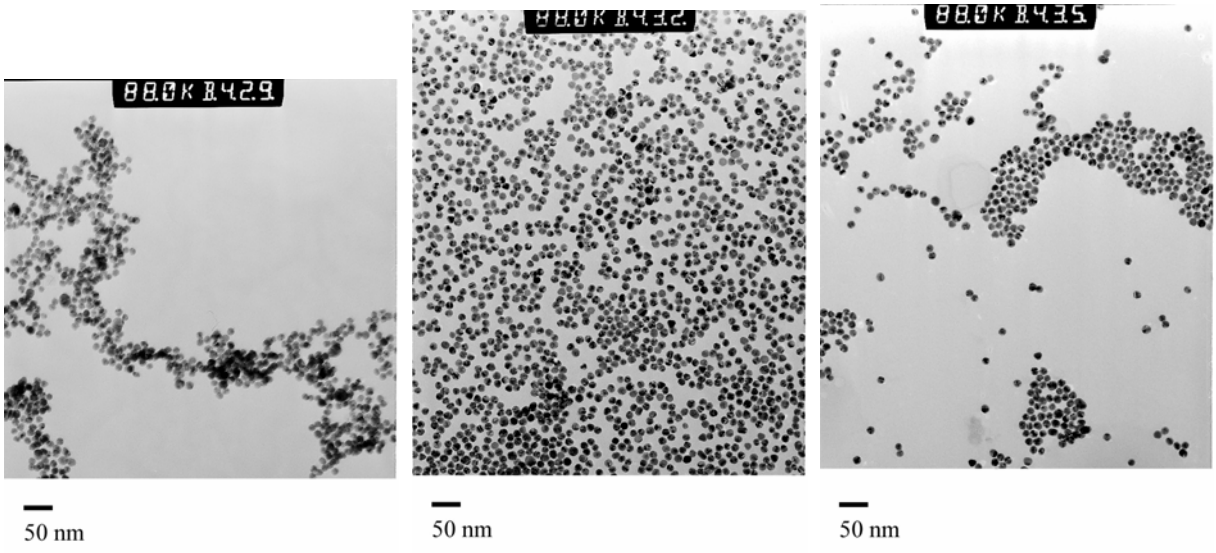

TEM measurements were performed by Inger Jensen at the Nano-Science Center, University of Copenhagen. Size distribution analyses were performed by measurement of 100 particles of each material.

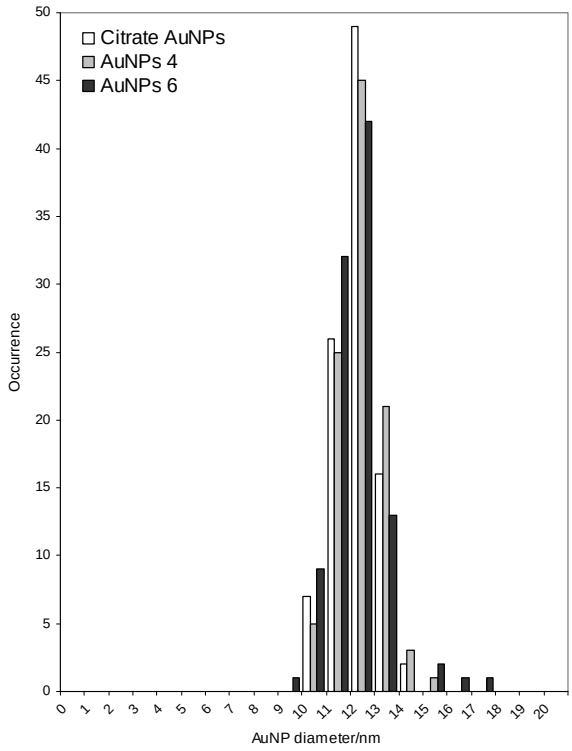

IX) UV-Vis spectra and kinetics of lectin-induced nanoparticle aggregation of AuNPs 9(conditions I) and kinetics of lectin-induced nanoparticle aggregation.

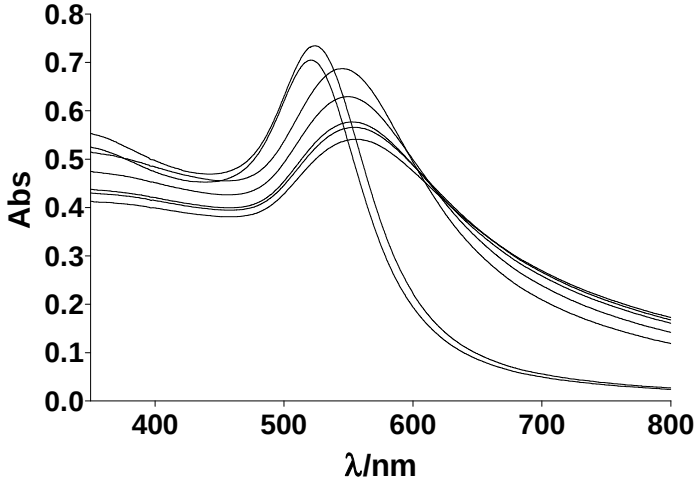

Overlay of UV-Vis spectra showing the red-shift and broadening of the SP band of maltose-conjugated glyconanoparticles **9**(conditions I) upon addition of Con A over 4 hours (0, 0.01, 0.5, 1, 2, 3, 4 hour spectra with maxima at increasing wavelengths are shown). All surface plasmon band shift values, $\Delta\lambda_{SP}$, of lectin-induced aggregation followed apparent first order kinetic profiles in $\Delta\lambda_{SP}$, which allowed the determination of the apparent first order rate constant, k_{obs}, and the maximal surface plasmon band shift, $\Delta\lambda_{SP,max}$, to describe the aggregation process under a given set of conditions. Hence, the equation

$$\Delta\lambda_{SP} = \Delta\lambda_{SP,max} \cdot \left(1 - e^{-k_{obs} \cdot t}\right)$$

was fitted to $\Delta\lambda_{SP}$ values, which in all cases provided squared correlation coefficients (R^2) above 0.98.

X) Detection limit of Con A-induced nanoparticle aggregation of AuNPs 9(conditions I).

A detailed study to determine the detection limit of lectin-induced nanoparticle aggregation was performed with Con A and AuNPs **9**(condition I) by varying lectin concentration (100 μM-10 nM), nanoparticle concentration (5 nM unless otherwise stated), and assay time (4, 20, or 48 h). Experiments were performed in triplicate and provided low relative standard deviations (RSD<0.4 nm) for all conditions.

Entry	$C_{Con\ A}$ (nM)	Time (h)	$\Delta\lambda_{SP,\ mean}$ (nm)	RSD (nm)	P value
1	100000	4	8.0	0.3	<0.0001
2	10000	4	23.5	0.3	<0.0001
3	1000	4	27.2	0.2	<0.0001
4	100	4	0.8	0.2	0.0074
5[a]	100	4	1.0	0.3	0.0255
6	100	20	1.0	0.3	0.0255
7[a]	100	20	2.3	0.2	0.0002
8	100	48	1.0	0.3	0.0255
9[a]	**100**	**48**	**2.8**	**0.2**	**<0.0001**
10	10	4	0	-	ns[b]
11[a]	10	4	0	-	ns[b]
12	10	48	0	-	ns[b]
13[a]	10	48	0	-	ns[b]

[a] 0.5 nM AuNPs. [b] ns: no significant shift

The detection limit was below 100 nM (entry 9) but above 10 nM Con A (entries 10-13). Assay sensitivity was to some extent enhanced at lower (0.5 μM) nanoparticle concentration. At higher lectin concentrations (100 μM, entry 1) where glyconanoparticles become saturated with protein, the lowered surface plasmon band shift (relative to entries 2 and 3) reflects a non-crosslinking surface plasmon resonance response.

XI) NMR spectra of compounds 2-Tr, 2 and 5.

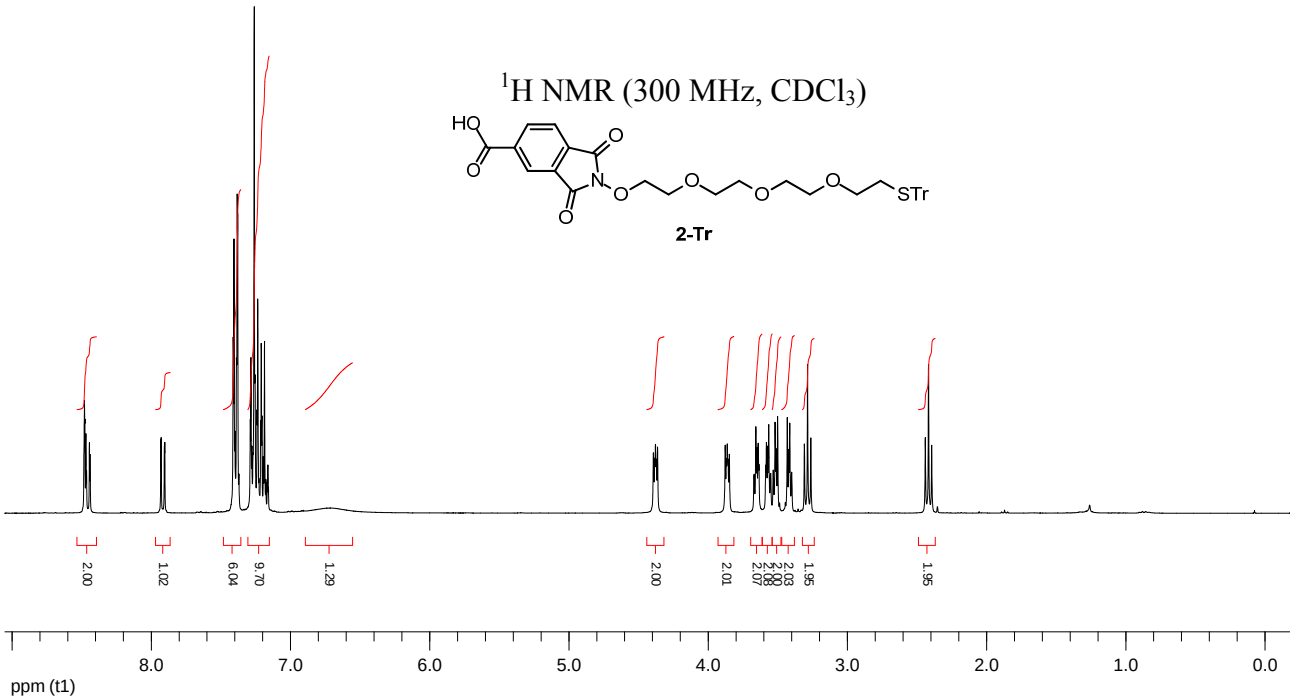

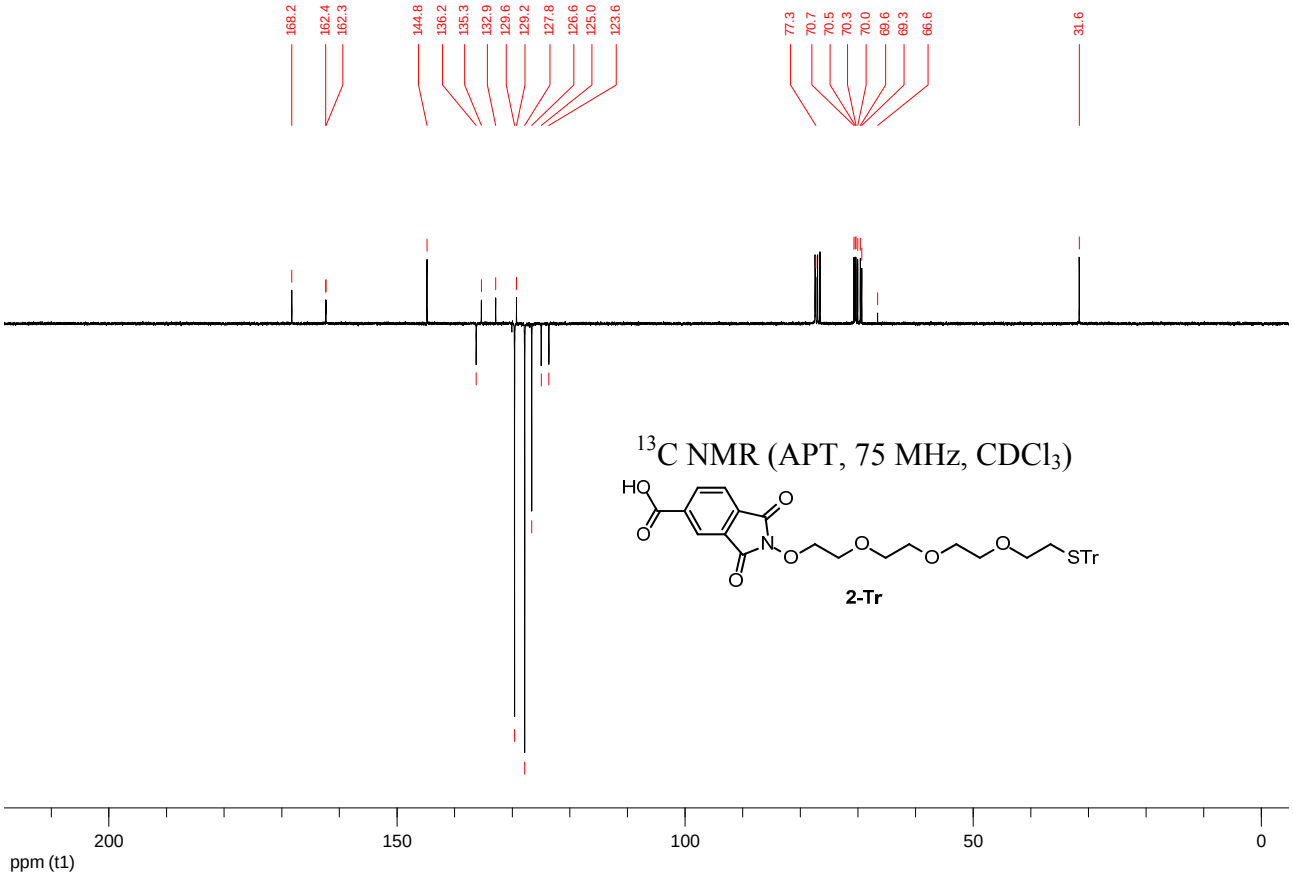

^{1}H NMR (300 MHz, $CDCl_3$)

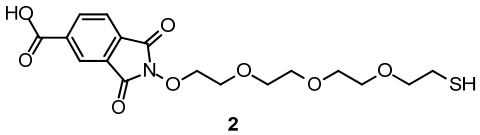

2

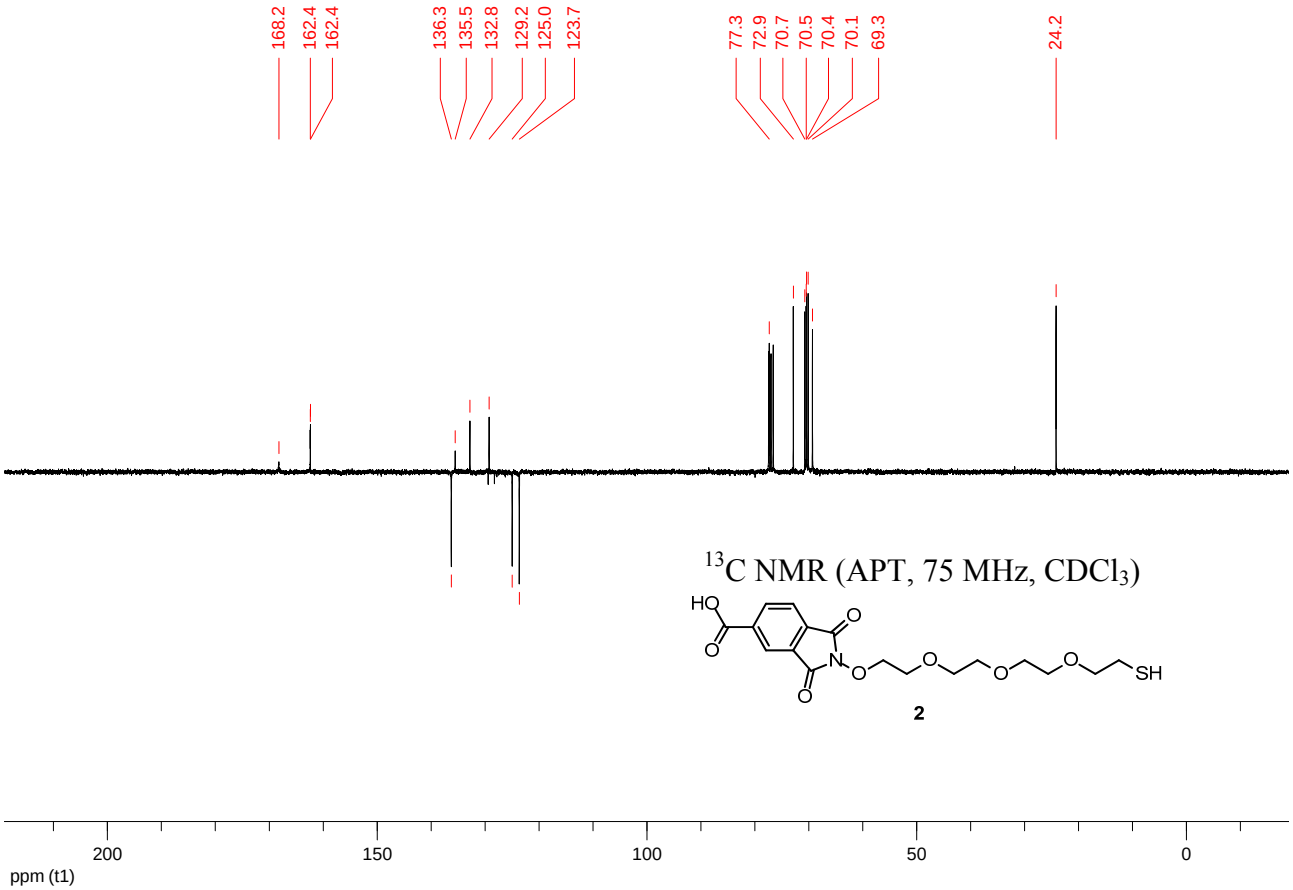

^{13}C NMR (APT, 75 MHz, $CDCl_3$)

2

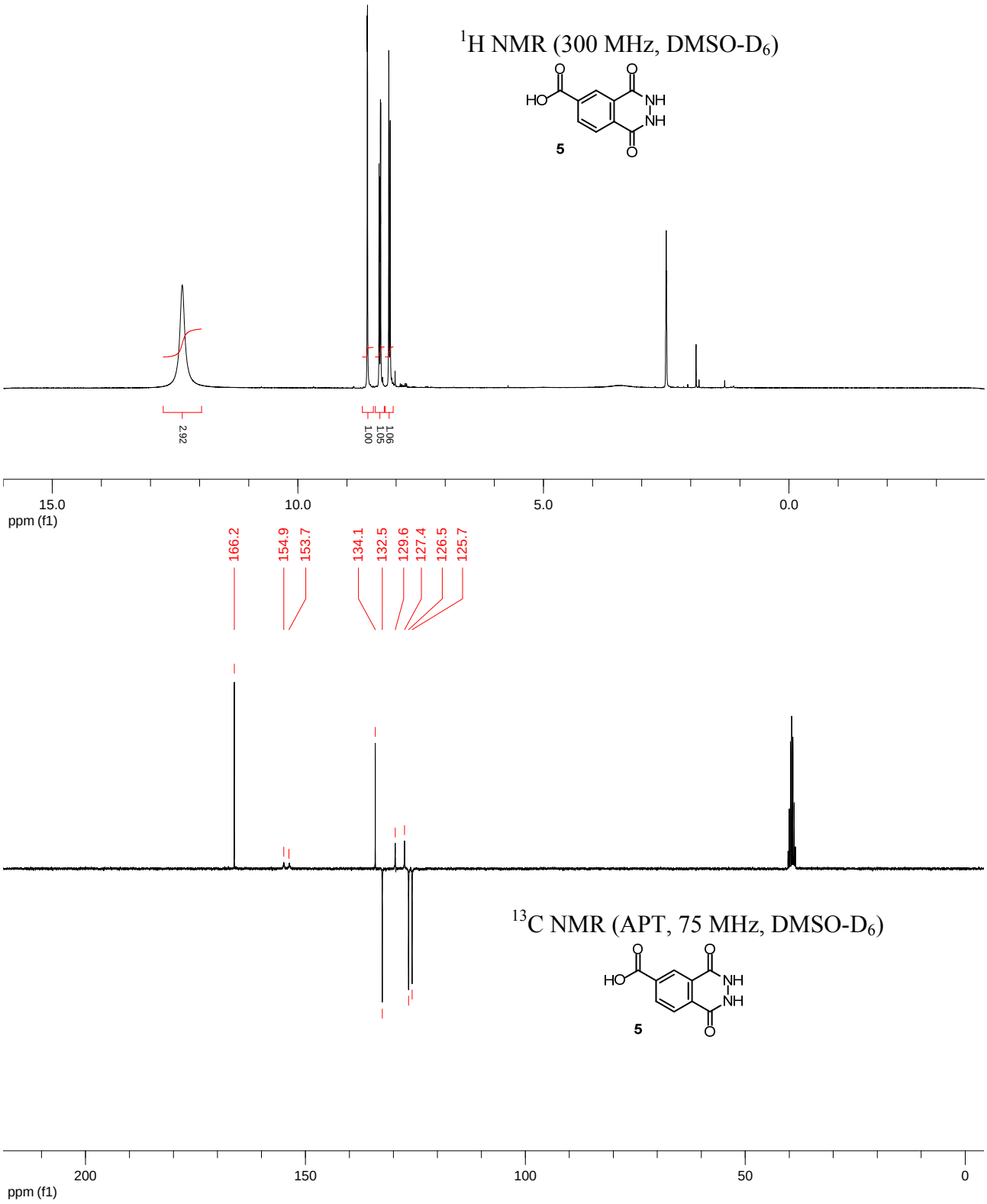
^{1}H NMR (300 MHz, DMSO-D$_6$)
HO
NH
NH
5
2.92
1.00
0.95
1.06
15.0
10.0
5.0
0.0
ppm (f1)
166.2
154.9
153.7
134.1
132.5
129.6
127.4
126.5
125.7
^{13}C NMR (APT, 75 MHz, DMSO-D$_6$)
HO
NH
NH
5
200
150
100
50
0
ppm (f1)

References

[S1] J. Brask, K. J. Jensen, *J. Peptide Sci.*, 2000, **6**, 290; F. Guillaumie, J. C. Kappel, N. M. Kelly, G. Barany, K. J. Jensen, *Tetrahedron Lett.*, 2000, **41**, 6131.

[S2] M. B. Thygesen, J. Sauer, K. J. Jensen, *Chem. Eur. J.*, 2009, **15**, 1649.